Mon. Not. R. Astron. Soc. **304,** 793–799 (1999)

A hybrid symplectic integrator that permits close encounters between massive bodies

J. E. Chambers
Armagh Observatory, Armagh BT61 9DG

Accepted 1998 December 2. Received 1998 November 25; in original form 1998 August 14

ABSTRACT

Mixed-variable symplectic integrators exhibit no long-term accumulation of energy error, beyond that owing to round-off, and they are substantially faster than conventional *N*-body algorithms. This makes them the integrator of choice for many problems in Solar system astronomy. However, in their original formulation, they become inaccurate whenever two bodies approach one another closely. This occurs because the potential energy term for the pair undergoing the encounter becomes comparable to the terms representing the unperturbed motion in the Hamiltonian. The problem can be overcome using a hybrid method, in which the close encounter term is integrated using a conventional integrator, whilst the remaining terms are solved symplectically. In addition, using a simple separable potential technique, the hybrid scheme can be made symplectic even though it incorporates a non-symplectic component.

Key words: accretion, accretion discs – methods: numerical – celestial mechanics, stellar dynamics – Solar system: general.

1 INTRODUCTION

Symplectic integrators have two key advantages over other *N*-body integrators: they exhibit no long-term build-up of energy error, and they are substantially faster for problems in which most of the mass is contained in a single body. This makes them well suited for studying a wide variety of problems in dynamical astronomy, especially those involving planetary or satellite systems.

The desirable energy conservation property arises because a symplectic integrator exactly solves the equations of motion for a problem very similar to the one in question. The high efficiency comes from the fact that the dominant force on each object can be 'built in', leaving only the smaller perturbations to constrain the size of the time-step. This means that a symplectic integrator needs to evaluate the forces acting on a body less often than conventional algorithms for the same level of accuracy.

In a seminal paper, Wisdom & Holman (1991) describe a simple second-order symplectic integrator, subsequently popularized by Levison and Duncan in their SWIFT integration package (Levison & Duncan 1994). This is roughly an order of magnitude faster than conventional integrators when applied to problems such as the long-term evolution of the planets. Higher order symplectic integrators also exist (Yoshida 1990), although these are usually no more efficient than the second-order method, since the increase in accuracy is offset by the extra computation required at each step.

Since then, a number of improvements have been made. The basic algorithm requires a fixed step-size, but it is possible to give each body in the integration a different fixed step-size (Saha & Tremaine 1994). This yields an extra gain in efficiency when the bodies have a wide range of orbital periods. Weak dissipative forces can also be included (Malhotra 1994; Cordeiro, Gomes & Martins 1997; Mikkola 1998), although strictly speaking this violates the symplectic properties of the integrator. In addition, at least two ways have been found to improve the accuracy of long-term integrations by making small changes to the variables prior to the start of the calculation (Saha & Tremaine 1992; Wisdom, Holman & Touma 1996). Mikkola (1997) describes a time transformation that overcomes the problem of using a fixed time-step to integrate orbits with high eccentricities.

The theory of symplectic integrators is described in a short review by Yoshida (1993), and in more detail by Sanz-Serna (1991).

The fixed time-step inherent in symplectic algorithms makes dealing with close encounters particularly difficult. Ideally one would like the step-size to decrease during an encounter in order to preserve the accuracy of the overall integration. However, changing the step-size of a symplectic integrator introduces an error with each change. If close encounters do not occur too often, this technique can still be used when the results of the integration are interpreted in a statistical sense (Levison & Duncan 1994). However, such an integrator cannot be relied upon to reproduce the true orbital evolution of a particular body (Michel & Valsecchi 1997).

One solution to this problem is to split up the perturbation terms, and give each part a separate (fixed) step-size, in such a way that stronger perturbations have smaller step-sizes (Duncan, Levison & Lee 1998). The resulting integrator, SYMBA, is truly symplectic, although it is rather cumbersome to implement in practice, and it may not retain the great speed advantage of the basic symplectic method.

In this paper, I describe an alternative solution – a hybrid integrator that melds symplectic and non-symplectic components

in such a way that the combined algorithm retains the desirable properties of both. The integrator was originally designed to study planetary accretion problems, which are characterized by repeated close encounters between large numbers of massive bodies. However, the principles involved are general, and the technique should be applicable to other problems.

In the next section I outline the theory behind symplectic integrators from a Lie series viewpoint. Symplectic integrators can also be understood in terms of the averaging principle, described by Wisdom & Holman (1991). Section 3 shows how the standard algorithm can be extended to include the effects of close encounters, using a hybrid integrator. Section 4 addresses the practical details of how to make such a scheme work. In Section 5, I put the hybrid integrator through its paces in a set of test problems. Finally, Section 6 explains how to obtain a copy of MERCURY, a publicly available software package that includes a working version of the integrator described here.

2 THE THEORY OF SYMPLECTIC INTEGRATORS

The basic theory of symplectic integrators can be understood by starting with Hamilton's equations of motion. These give the rate of change of the position, x, and momentum, p, for each object in an N-body system:

$$\frac{\mathrm{d}x_i}{\mathrm{d}t} = \frac{\partial H}{\partial p_i},$$
$$\frac{dp_i}{\mathrm{d}t} = -\frac{\partial H}{\partial x_i}. \quad (1)$$

The Hamiltonian, H, is the sum of the kinetic and potential energy terms for all the bodies:

$$H = \sum_{i=1}^{N} \frac{p_i^2}{2m_i} - G\sum_{i=1}^{N} m_i \sum_{j=i+1}^{N} \frac{m_j}{r_{ij}},$$

where m_i is the mass of body i, and r_{ij} is the separation between bodies i and j. Using equations (1), the rate of change of any quantity, q, can be expressed as

$$\begin{aligned}\frac{\mathrm{d}q}{\mathrm{d}t} &= \sum_{i=1}^{n}\left(\frac{\partial q}{\partial x_i}\frac{\mathrm{d}x_i}{\mathrm{d}t} + \frac{\partial q}{\partial p_i}\frac{\mathrm{d}p_i}{\mathrm{d}t}\right)\\ &= \sum_{i=1}^{n}\left(\frac{\partial q}{\partial x_i}\frac{\partial H}{\partial p_i} - \frac{\partial q}{\partial p_i}\frac{\partial H}{\partial x_i}\right)\\ &= Fq, \end{aligned} \quad (2)$$

where F is an 'operator'. The variable q can represent the position or momentum of a body, or any combination of x and p for all the bodies. The general solution of equation (2) at time t is

$$\begin{aligned} q(t) &= \mathrm{e}^{\tau F} q(t-\tau)\\ &= \left(1 + \tau F + \frac{\tau^2 F^2}{2} + \ldots\right) q(t-\tau), \end{aligned}$$

where $q(t-\tau)$ is the value of q at an earlier epoch.

So far, all we have done is rewrite the equations of motion, and these remain insoluble analytically, except in special cases. The trick of symplectic integrators is to split H into pieces, each of which can be solved on its own, and then apply the solutions one at a time in such a way that they approximate the solution of the problem as a whole.

For example, let $H = H_A + H_B$. The time evolution of q is now given by

$$q(t) = \mathrm{e}^{\tau(A+B)} q(t-\tau), \quad (3)$$

where A and B are new operators, such that

$$A = \sum_{i=1}^{n}\left(\frac{\partial}{\partial x_i}\frac{\partial H_A}{\partial p_i} - \frac{\partial}{\partial p_i}\frac{\partial H_A}{\partial x_i}\right)$$

with an analogous expression for B. These operators obey many of the usual rules of algebra, with an important exception: we cannot assume that they commute. In other words $AB \neq BA$, in general. Bearing this in mind, the exponential in equation (3) can be expanded to give

$$\begin{aligned} \mathrm{e}^{\tau(A+B)} &= 1 + \tau(A+B) + \frac{\tau^2(A+B)^2}{2} + \ldots\\ &= 1 + \tau(A+B) + \frac{\tau^2(A^2 + AB + BA + B^2)}{2} + \ldots. \end{aligned} \quad (4)$$

Now consider the result of applying the exponential operators one after the other:

$$\begin{aligned} \mathrm{e}^{\tau A}\mathrm{e}^{\tau B} &= \left(1 + \tau A + \frac{\tau^2 A^2}{2} + \ldots\right)\left(1 + \tau B + \frac{\tau^2 B^2}{2} + \ldots\right)\\ &= 1 + \tau(A+B) + \frac{\tau^2(A^2 + 2AB + B^2)}{2} + \ldots. \end{aligned} \quad (5)$$

Note that the right-hand sides of equations (4) and (5) are the same to $O(\tau)$.

Applying one of the exponential operators on its own is equivalent to solving the equations of motion with only the corresponding part of the Hamiltonian present. There are several ways of splitting H into two parts, each of which can be integrated efficiently. Often, the best approach is to choose two parts that are each soluble analytically. However, this is not necessary if there is an efficient way to integrate H_A and H_B numerically.

Whichever way we choose to split the Hamiltonian, a first-order integrator is given by

$$q(t) = \mathrm{e}^{\tau A}\mathrm{e}^{\tau B} q(t-\tau),$$

where τ is the step-size. Each step of the integrator consists of two substeps:

(i) advance the system subject to the forces associated with H_B for one time-step (ignoring the effect of H_A);

(ii) advance the resulting system subject to the forces associated with H_A for one time-step.

Splitting the $\exp(\tau B)$ term in half gives a second-order integrator:

$$q(t) = \mathrm{e}^{\tau B/2}\mathrm{e}^{\tau A}\mathrm{e}^{\tau B/2} q(t-\tau), \quad (6)$$

which is equivalent to equation (3) to $O(\tau^2)$. Higher order integrators can be devised by splitting each of the exponential terms still further (Yoshida 1990).

Using any of these integrators is equivalent to exactly solving the equations of motion for a system with Hamiltonian H_{integ}, which is close to that of the real problem. For example, for the first-order integrator:

$$H_{\mathrm{integ}} = H + \frac{\tau}{2}\sum_{i=1}^{n}\left(\frac{\partial H_B}{\partial x_i}\frac{\partial H_A}{\partial p_i} - \frac{\partial H_B}{\partial p_i}\frac{\partial H_A}{\partial x_i}\right) + O(\tau^2) \quad (7)$$

(Saha & Tremaine 1992). H_{integ} is conserved exactly, to within computer round-off error. So, if τ is small, H will differ from H_{integ} by only a small amount, and there will be no long-term build-up in the energy error.

The error incurred at each step of an integrator can be expressed in terms of A and B. For the first-order integrator

$$\mathrm{e}^{\tau A}\mathrm{e}^{\tau B} = \mathrm{e}^{\tau(A+B)} + \frac{\tau^2}{2}(AB - BA) + \ldots.$$

If we continued to work out the higher order terms in this expression, we would find that all of them depend on both A and B. This means that if $B \sim \epsilon A$, where ϵ is a small quantity, the error per step will also be proportional to ϵ. For this reason it pays to split the Hamiltonian into a dominant part plus a small perturbation if possible. In the case of the Solar system, the dominant force is usually due to the gravity of the Sun, so we can assign H_A and H_B as follows.

H_A: each body moves on an unperturbed Keplerian orbit about the Sun.

H_B: each body remains fixed, and receives an acceleration owing to perturbations from the other bodies.

The precise details of how this is done depend on the variables chosen. Using barycentric coordinates, $H_A \gg H_B$ for all the bodies orbiting the Sun, but not for the Sun itself, so the error per step no longer benefits from the ϵ factor. Wisdom & Holman (1991) advocate using Jacobi variables, and this works satisfactorily. However, for reasons that will become apparent later, it is better to use mixed-centre variables (called 'democratic heliocentric' variables by Duncan et al. 1998). These consist of heliocentric coordinates and barycentric velocities, which also satisfy Hamilton's equations.

Using mixed-centre coordinates, the Hamiltonian can be split as follows:

$$
\begin{aligned}
H_A &= \sum_{i=1}^{N}\left(\frac{p_i^2}{2m_i} - \frac{Gm_\odot m_i}{r_{i\odot}}\right),\\
H_B &= -G\sum_{i=1}^{N}\sum_{j=i+1}^{N}\frac{m_i m_j}{r_{ij}},\\
H_C &= \frac{1}{2m_\odot}\left(\sum_{i=1}^{N}\boldsymbol{p}_i\right)^2,
\end{aligned}
\tag{8}
$$

where N now refers to the number of objects not including the Sun, and quantities with the index $\odot$ refer to the Sun. Note that each of these partial Hamiltonians can be solved analytically in the absence of the others.

One minor drawback with using mixed-centre coordinates is that, in addition to H_A and H_B, the terms arising from the kinetic energy of the Sun have to be placed in a third part of the Hamiltonian, H_C. However, the ideas outlined above can be easily extended to handle this situation. For example, the second-order integrator in equation (6) now becomes

$$q(t) = \mathrm{e}^{\tau B/2}\mathrm{e}^{\tau C/2}\mathrm{e}^{\tau A}\mathrm{e}^{\tau C/2}\mathrm{e}^{\tau B/2}q(t-\tau),$$

where the operator C arises from the Hamiltonian H_C.

Provided that all the bodies remain far apart from one another, $H_A \gg H_B$, and $H_A \gg H_C$. This means that each step of the integrator has an error of $O(\epsilon\tau^3)$, where $\epsilon = \sum m_i/m_\odot$. However, if two bodies undergo a close approach (that is, r_{ij} becomes small), the corresponding term in H_B becomes large, and the error per step increases substantially. This is the reason why, until recently, symplectic integrators have been unable to address a large class of problems in Solar-system science – those involving small bodies on planet-crossing orbits, and accretion discs.

3 CLOSE ENCOUNTERS

Conventional integrators often reduce the size of the time-step during a close encounter, in order to maintain the same level of accuracy. However, each time the step-size, τ, of a symplectic integrator is changed, the integration Hamiltonian also changes (see equation 7). This produces a shift in the energy of the real system. If many close encounters occur, this energy error builds up, and eventually destroys the symplectic property of the integrator.

During an encounter between bodies α and β, their separation $r_{\alpha\beta}$ becomes small. This makes one of the terms in H_B comparable in size to H_A (see equations 8), and the error per step increases from $O(\epsilon\tau^3)$ to $O(\tau^3)$. This problem can be remedied if H_B can somehow be made small again compared with H_A. One way to do this is simply to transfer the term involving $r_{\alpha\beta}$ from H_B to H_A for the duration of the close encounter:

$$
\begin{aligned}
H_A &= \sum_{i=1}^{N}\left(\frac{p_i^2}{2m_i} - \frac{Gm_\odot m_i}{r_{i\odot}}\right) - \frac{Gm_\alpha m_\beta}{r_{\alpha\beta}},\\
H_B &= -G\sum_{i\neq\alpha}\sum_{j>i}\frac{m_i m_j}{r_{ij}} - G\sum_{j>\alpha}^{j\neq\beta}\frac{m_\alpha m_j}{r_{\alpha j}}.
\end{aligned}
$$

H_A is no longer integrable analytically, since it contains the three-body problem of the Sun plus objects α and β. However, this is not really a problem in practice, as these terms can be integrated numerically, at close to machine precision, using a conventional N-body integrator.

At this point, the advantage of using mixed-centre coordinates rather than Jacobi coordinates becomes apparent. Using mixed-centre coordinates, all of the Kepler terms in H_A can still be advanced analytically, except for objects α and β. Using Jacobi coordinates, H_A becomes

$$H_A = \sum_{i=1}^{N}\left(\frac{\tilde{p}_i^2}{2m_i} - \frac{Gm_\odot m_i}{\tilde{r}_i}\right) - \frac{Gm_\alpha m_\beta}{r_{\alpha\beta}},$$

where Jacobi coordinates are indicated by tildes, and

$$\boldsymbol{r}_{\alpha\beta} = \boldsymbol{r}_\beta - \boldsymbol{r}_\alpha = \tilde{\boldsymbol{r}}_\beta - \tilde{\boldsymbol{r}}_\alpha + \sum_{j=\alpha}^{\beta-1}\frac{m_j\tilde{\boldsymbol{r}}_j}{m_\odot + \sum_{k=1}^{j} m_k}.$$

Now, in addition to integrating terms involving α and β numerically, all terms involving bodies with indices $\alpha < j < \beta$ have to be integrated numerically as well. Clearly, Jacobi coordinates are not the ones to use when close encounters can occur, and we will stick with mixed-centre coordinates.

The scheme described above is easy to implement and works fairly well. However, moving terms between H_A and H_B at each close encounter still involves changing H_{integ}, albeit not by as much as changing the step-size. To keep H_{integ} constant, and make the hybrid integrator truly symplectic, we need to ensure that terms never have to be transferred between different parts of the Hamiltonian. We can do this by splitting each of the interaction terms between H_A and H_B in such a way that the part in H_B always remains small, while the part in H_A is only evaluated during a close encounter:

$$
\begin{aligned}
H_A &= \sum_{i=1}^{N}\left(\frac{p_i^2}{2m_i} - \frac{Gm_\odot m_i}{r_{i\odot}}\right)\\
&\quad - G\sum_{i=1}^{N}\sum_{j=i+1}^{N}\frac{m_i m_j}{r_{ij}}[1 - K(r_{ij})],\\
H_B &= -G\sum_{i=1}^{N}\sum_{j=i+1}^{N}\frac{m_i m_j}{r_{ij}}K(r_{ij}).
\end{aligned}
\tag{9}
$$

Fig. 1 shows a suitable form for K. When r_{ij} is large, K should tend to one, while tending to zero when r_{ij} is small. This ensures that $H_B \ll H_A$, even during a close encounter. In the absence of an encounter, the terms in H_A can be advanced analytically as before.

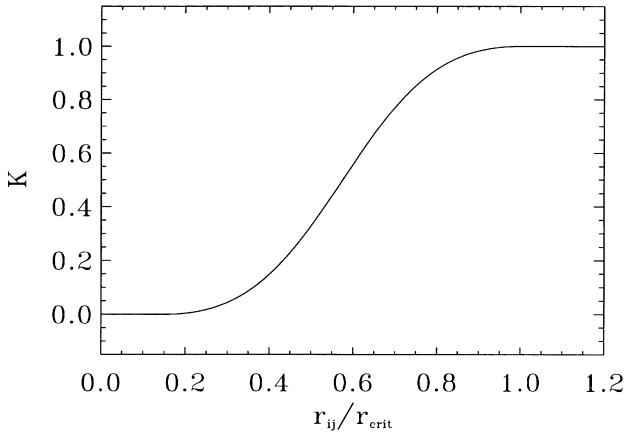

Figure 1. A suitable form for the changeover function K, as a function of the separation, r_{ij}, between two bodies.

This solution was inspired by the separable potential method of Duncan et al. (1998), but here the potential terms need only be split into two pieces rather than many.

As with the standard symplectic integrator, there is no guarantee that the terms in equation (7) will converge for the hybrid integrator. There may be cases where the series diverges, producing errors that are larger than suggested by the leading term [which is $O(\epsilon\tau^3)$ for the second-order integrator]. I plan to investigate this possibility further in a later paper.

The integration scheme for the second-order hybrid integrator is as follows.

(i) The coordinates remain fixed. Each body receives an acceleration owing to the other bodies (but not the Sun), weighted by a factor $K(r_{ij})$, lasting for $\tau/2$.

(ii) The momenta remain fixed, and each body shifts position by an amount $\tau \sum_i \boldsymbol{p}_i/2m_\odot$.

(iii) Bodies not in an encounter move on a Keplerian orbit about the Sun for τ. For bodies in an encounter, the Kepler terms, and the close encounter terms weighted by $(1 - K)$, are integrated numerically for τ.

(iv) As step (ii).

(v) As step (i).

4 PRACTICAL DETAILS

4.1 The changeover function

The integration scheme outlined above is all very well in theory, but several details need to be addressed before it will work in practice. The first of these is the form of the changeover function, K, used to switch between the standard symplectic scheme and the close encounter regime. This function has to meet several criteria:

(i) $K \rightarrow 1$ when r_{ij} is large, and $K \rightarrow 0$ when r_{ij} is small;

(ii) K is smooth enough that the numerical algorithm can follow it without difficulty;

(iii) K can be evaluated quickly.

After some trial and error, I have found that the following expression works well:

$$K = \begin{cases} 0, & \text{for } y < 0 \\ y^2/(2y^2 - 2y + 1) & \text{for } 0 < y < 1, \\ 1 & \text{for } y > 1, \end{cases} \quad (10)$$

where

$$y = \left(\frac{r_{ij} - 0.1\, r_{\rm crit}}{0.9\, r_{\rm crit}} \right)$$

and $r_{\rm crit}$ is a free parameter.

One might object that the derivatives of equation (10) have discontinuities at $y = 0$ and 1, and that these could cause problems. However, the non-symplectic integrator will only sample the function at a finite (often small) number of points, so it is merely necessary to fool the integrator into thinking that the function is smooth. Equation (10) seems to avoid difficulties unless the numerical algorithm is used with a very strict tolerance, combined with a small step-size for the symplectic integrator.

4.2 The changeover distance

The value of the critical distance, $r_{\rm crit}$, at which the numerical algorithm starts to integrate a close encounter is something of a compromise. If $r_{\rm crit}$ is too small, the encounter will not be calculated properly. If $r_{\rm crit}$ is too large, then the computer time needed to follow the encounter will be more than can be justified by the overall accuracy of the integration.

Levison & Duncan (1994) take special steps to deal with close encounters when $r_{ij} < 3R_{\rm H}$, where $R_{\rm H}$ is the Hill radius. Duncan et al. (1998) recommend a value of 3 mutual Hill radii for encounters involving two massive bodies. These values seem to work well when one or both of the objects are large (comparable in mass to the giant planets). However, when the masses are smaller, the key factor is not the number of Hill radii, but rather the number of time-steps used to sample the changeover function K. A pair of objects with lunar mass can easily travel 3 mutual Hill radii in a single time-step. In this case the switch from the symplectic regime to the hybrid regime would be instantaneous, leading to large errors during the close encounter.

For this reason I advocate a two-fold strategy. For each object, $r_{\rm crit}$ should be the larger of $n_1 R_{\rm H}$ and $n_2 \tau v_{\rm max}$, where n_1 and n_2 are parameters, and $v_{\rm max}$ is the maximum velocity expected during the integration (say, the initial orbital velocity of the innermost body). During a particular encounter, $r_{\rm crit}$ should be the larger of the values for the two bodies involved. The precise values of n_1 and n_2 used will depend on the nature of the problem being studied, but values in the ranges $n_1 = 3$–10 and $n_2 = 0.3$–2.0 seem to cover most likely cases.

4.3 Which numerical integrator?

The N-body algorithm used to integrate the close encounters numerically is a matter of personal preference. The Bulirsch–Stoer method (Stoer & Bulirsch 1980) is often used to check the results of other integration algorithms, since it is generally robust for N-body problems. For this reason I advocate using it here. The standard version assumes that the force on each object can be a function of both the coordinates and momenta. Press et al. (1992) give a version designed for conservative systems (where the force is a function of x only), based on Stoermer's rule, and this is about twice as fast as the standard algorithm. Everhart's RADAU routine (Everhart 1985) is faster still, but it occasionally runs into difficulty when objects undergo very close encounters, so it is probably safer to use Bulirsch–Stoer.

4.4 Predicting encounters

Prior to calculating each step, the hybrid integrator needs to know

which bodies will be involved in a close encounter at some point during the step. It is not sufficient to check the separation of each pair of objects at the start and end of the step, since this may miss a separation minimum occurring in between. For this reason I recommend including some sort of predictor step in the integrator. This need not be particularly accurate, as long as it errs on the side of caution. For example, if the predictor indicates an encounter that never actually takes place, the worst that will happen is that the Keplerian motion of these objects will be calculated using the numerical routine instead of analytically.

One way to do the prediction is to advance each object (as crudely as one dares) forward for one time-step along a Keplerian orbit about the Sun. Only objects far from an encounter need be checked this way, so the Keplerian approximation is a reasonable one. Armed with the initial and final coordinates and momenta of each body, we can interpolate to get an expression for the separation, $\Delta = r_{ij}$, of any pair accurate to $O(\tau^3)$:

$$\Delta = (1-t)^2(1+2t)\Delta_0 + t^2(3-2t)\Delta_1 + t(1-t)^2\tau\dot{\Delta}_0 - t^2(1-t)\tau\dot{\Delta}_1, \quad (11)$$

where Δ_0, Δ_1 are the separations at the start and end of the prediction step, respectively, and $\dot{\Delta}_0$, $\dot{\Delta}_1$ are the time derivatives of the separation (which can also be found from $\boldsymbol{x}$ and $\boldsymbol{p}$). Also, t is normalized time, such that $t = 0$ at the start of the step, and $t = 1$ at the end of the step.

Setting the derivative of equation (11) equal to zero, we get an expression for t when the separation is a minimum:

$$at^2 + bt + c = 0,$$

where

$$a = 6(\Delta_0 - \Delta_1) + 3\tau(\dot{\Delta}_0 + \dot{\Delta}_1),$$
$$b = 6(\Delta_1 - \Delta_0) - 2\tau(2\dot{\Delta}_0 + \dot{\Delta}_1),$$
$$c = \tau\dot{\Delta}_0.$$

Equation (11) then gives the minimum separation of the pair of objects.

This procedure, combined with a 'pre-checker' that eliminates pairs of objects that cannot possibly undergo an encounter during the next step, takes only a few per cent of the total computer time for an integration. Higher order interpolation schemes can be derived by calculating the accelerations (owing to the Sun) at the start and end of the prediction step. However, these have an unfortunate habit of giving spurious additional minima, so the cubic interpolation given above is probably best. Finally, I note that the same interpolation scheme can applied after the real integration step, to estimate the minimum separation of objects undergoing a close encounter.

5 TEST INTEGRATIONS

5.1 Scaled outer Solar system

Duncan et al. (1998) tested their SYMBA symplectic algorithm by integrating the orbits of the four giant planets, with masses enhanced by a factor of 50. This configuration is unstable, and the planets quickly began to have close encounters with one another. Shortly afterwards, two of the planets were ejected from the system.

Here, I repeat their calculation using the hybrid algorithm. The integration uses $\tau = 11.05$ d and $r_{\rm crit} = 3R_{\rm H}$, similar to the values used by Duncan et al. Fig. 2 shows the evolution of the relative energy error $\Delta E = (E - E_0)/E_0$, where E and E_0 are the energy at time t and the initial energy respectively. The energy error is similar

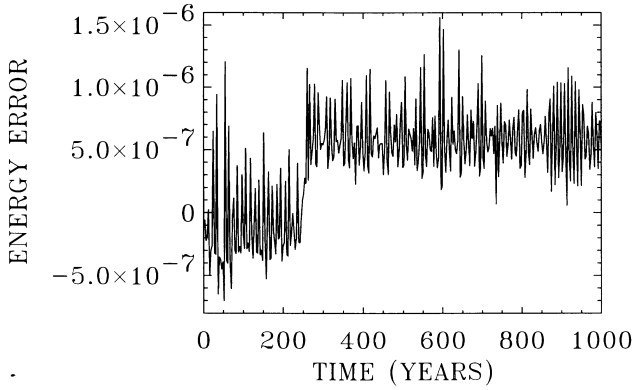

Figure 2. Relative energy error during an integration of the four giant planets, with masses enhanced by a factor of 50, using the hybrid integrator.

to that using the SYMBA integrator, even allowing for the jump at $t \sim 250$ yr, caused by an exceptionally close encounter between Jupiter and Saturn to within 0.007 au.

The time evolution of the orbits of the planets is highly chaotic, so the evolution differs from the integration of Duncan et al. In fact, even small changes in the step-size produce a different outcome. The value of τ used here was chosen to maximize the time of first ejection, which occurs at about 1000 yr, when Neptune is removed. Shortly afterwards both Uranus and Saturn are ejected, leaving only Jupiter on a bound orbit.

5.2 The restricted three-body problem

The restricted three-body problem consists of two massive bodies moving on circular orbits, and a third massless particle. This has an integral of motion – the Jacobi constant, C. To test how well the integrator conserves C, I integrated 36 test particles initially on a ring outside the orbit of a planet with a mass and orbit similar to Neptune. The particles had semi-major axes $a = 36$ au, eccentricities $e = 0.18$, and mean anomalies, M, evenly spaced along their orbit. The corresponding elements for Neptune were $a = 30$ au, $e = 0$ and $M = 0$. All objects moved in the same orbital plane. The objects were integrated for 10^6 yr, with $\tau = 5$ yr, a Bulirsch–Stoer tolerance of 10^{-10} and $r_{\rm crit} = 10$ Hill radii $\sim$7.7 au.

During the integration, the maximum relative error on C was about 3×10^{-6}, a figure that was similar for all the objects. A Bulirsch–Stoer integration (using Stoermer's method) with tolerance of 10^{-9} gave similar results, requiring about 50 per cent more computer time.

5.3 Planetary embryos

The hybrid integrator was originally developed for planetary accretion problems, so here is a typical test case. 30 planetary embryos have initial semi-major axes $a = 0.5$–1.2 au, eccentricities $e = 0$–0.01 and inclinations $i = 0$. The remaining angular elements are randomly distributed. The embryo masses range from about 0.6 lunar masses to 0.2 Earth masses. The bodies are treated as point masses (collisions are ignored), with a gravitational smoothing length, $s = 3 \times 10^{-8}$ au $\sim$5 km, such that the usual expression for the force between two bodies is replaced by

$$\boldsymbol{F}_{ij} = -\frac{Gm_i m_j}{(r_{ij}^2 + s^2)}\frac{\boldsymbol{r}_{ij}}{r_{ij}}.$$

The embryos are integrated for 10 000 yr using the hybrid integrator,

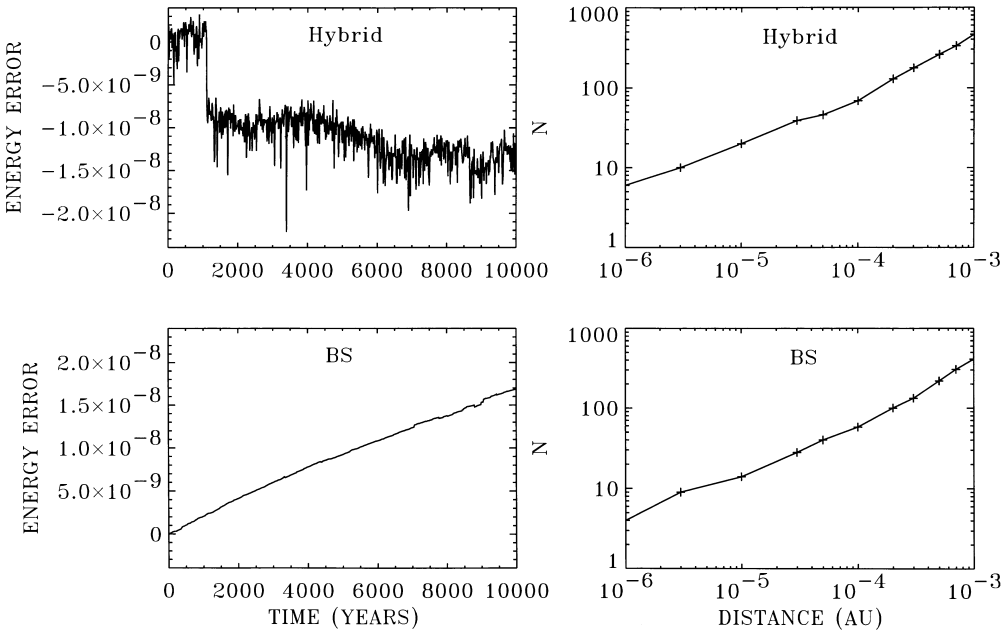

Figure 3. Relative energy error versus time for an integration of 30 planetary embryos, using the hybrid integrator and the Bulirsch–Stoer (BS) integrator. Also shown are the cumulative number of close encounters, N, as a function of distance of closest approach, for each integration.

with $\tau = 5$ d, a Bulirsch–Stoer tolerance of 10^{-12}, and $r_{\rm crit} = 0.5\tau v_{\rm max} \sim 0.06$ au. Since the problem is two-dimensional, a large number of close encounters can be expected during the integration.

Fig. 3 shows the evolution of the energy error during the integration. For comparison, the figure also shows the energy error for the same calculation using the Stoermer version of the Bulirsch–Stoer algorithm, with a tolerance of 10^{-10}. The maximum energy error is about the same in each case, although the Bulirsch–Stoer integration takes 3.5 times longer. The energy error shows a linear increase with time in the Bulirsch–Stoer calculation. Using the hybrid integrator, the energy variations over short periods of time are much larger, but no secular trend is apparent.

Also shown in Fig. 3 is the cumulative number distribution of close encounters in each integration. The distributions have approximately the same slope, and the total number of encounters is similar.

Incidentally, using the SYMBA algorithm of Duncan et al. (1998), the final energy error for the same integration is about two orders of magnitude larger (Duncan, private communication), presumably because this algorithm uses a smaller value of $r_{\rm crit}$.

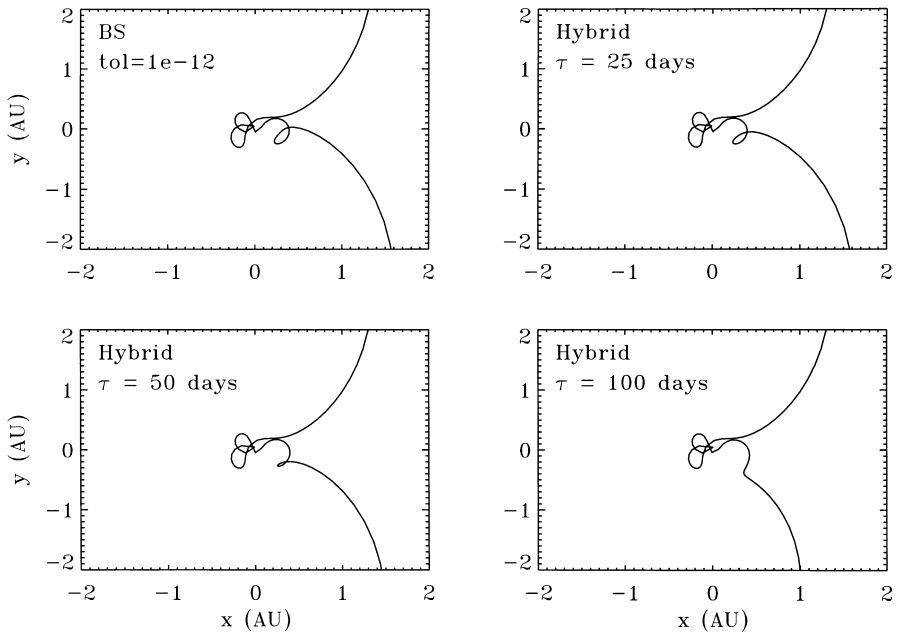

Figure 4. Trajectory of Comet P/Oterma during a close encounter with Jupiter, integrated using the Bulirsch–Stoer (BS) integrator and the hybrid integrator. The trajectory is shown in a rotating frame, with Jupiter at the origin and the Sun on the negative x-axis.

5.4 Comet P/Oterma

Michel & Valsecchi (1997) have shown that changing the time-step of a symplectic integrator can lead to spurious results. They integrated a close encounter between Comet P/Oterma and Jupiter, using the Bulirsch–Stoer method as a reference, and using the RMVS2 algorithm of Levison & Duncan (1994). The latter is based on a second-order symplectic integrator. During a close encounter it first decreases the step-size, and then changes the centre of motion to the planet instead of the Sun. This technique failed to reproduce the correct trajectory of the comet during the encounter if the time-step was larger than about 20 d.

We have to be sure that the hybrid integrator does not suffer from the same problem, so I have repeated the test here. The first panel of Fig. 4 shows the close encounter trajectory calculated using the Bulirsch–Stoer method, with a tolerance parameter of 10^{-12}. The coordinate origin is at Jupiter in a rotating frame, with the Sun on the negative x-axis. The initial conditions are those given in table IV of Michel & Valsecchi (1997). The second panel shows the trajectory calculated using the hybrid integrator, with a step-size of 25 d, and a changeover distance of 3 Hill radii (the same as used by RMVS2). The diagrams are virtually identical.

In fact, the hybrid integrator does quite well for larger step-sizes too. The evolution is qualitatively similar in the third panel (step-size 50 d). Even with a step-size of 100 d (fourth panel), the hybrid integrator does better than RMVS2 with a step-size four times smaller. Perhaps this is not too surprising, since the same Bulirsch–Stoer algorithm is doing all the hard work of getting the close encounter right regardless of the step-size. For this reason too, the time taken to complete the calculation is about the same for the hybrid as for Bulirsch–Stoer on its own. In order to see the inherent speed advantage of the symplectic part of the integrator, we would need to include more planets in the calculation.

6 THE MERCURY INTEGRATOR PACKAGE

The hybrid symplectic integrator described in this paper is included in a publicly available N-body integrator package called MERCURY (Chambers & Migliorini 1997). Copies of the source code, instructions for how to compile and run the programs, and example integrations can be obtained via anonymous FTP at Armagh Observatory (star.arm.ac.uk in the subdirectory pub/jec). In addition to the symplectic integrator, the package includes the Bulirsch–Stoer algorithms and a version of Everhart's RADAU integrator.

ACKNOWLEDGMENTS

I am very grateful to David Asher, Mark Bailey, Jacques Laskar, Seppo Mikkola, Alessandro Morbidelli, Scott Tremaine and especially Martin Duncan for helpful discussions and ideas during the preparation of this work.

REFERENCES

Chambers J. E., Migliorini F., 1997, BAAS, 29, 1024
Cordeiro R. R., Gomes R. S., Martins R. V., 1997, Celest. Mech., 65, 407
Duncan M., Levison H. F., Lee M. H., 1998, AJ, 116, 2067
Everhart E., 1985, in Carusi A., Valsecchi G. B., eds, Dynamics of Comets: Their Origin and Evolution. Reidel, Dordrecht, p. 185
Levison H. F., Duncan M. J., 1994, Icarus, 108, 18
Malhotra R., 1994, Celest. Mech., 60, 373
Michel P., Valsecchi G. B., 1997, Celest. Mech., 65, 355
Mikkola S., 1997, Celest. Mech., 67, 145
Mikkola S., 1998, Celest. Mech., 68, 249
Press W. H., Teukolsky S. A., Vetterling W. T., Flannery B. P., 1992, Numerical Recipes in Fortran, 2nd edn. Cambridge Univ. Press, Cambridge
Saha P., Tremaine S., 1992, AJ, 104, 1633
Saha P., Tremaine S., 1994, AJ, 108, 1962
Sanz-Serna J. M., 1991, Acta Num., (1991) p. 243
Stoer J., Bulirsch R., 1980, Introduction to Numerical Analysis. Springer-Verlag, New York
Wisdom J., Holman M., 1991, AJ, 102, 1528
Wisdom J., Holman M., Touma J., 1996, Fields Instit. Commun., 10, 217
Yoshida H., 1990, Phys. Lett. A, 150, 262
Yoshida H., 1993, Celest. Mech., 56, 27

This paper has been typeset from a TEX/LATEX file prepared by the author.